JOURNAL OF MATERIALS SCIENCE 23 (1988) 2745–2752

Carbon fibre reinforced glass matrix composite tension and flexure properties

KARL M. PREWO
United Technologies Research Center, East Hartford, Connecticut 06018, USA

Carbon fibre reinforced borosilicate glass matrix composites have been fabricated to determine their mechanical properties in tension and flexure. Composite tensile stress–strain properties, including elastic modulus, proportional limit and ultimate tensile strength, have been measured as a function of fibre content. Composite tensile properties were also obtained at temperatures of up to 625° C through the testing of 0/90 cross-plied specimens. Composite short-beam shear strength was found to depend on specimen orientation and also on the composition of the glass matrix. This compositional dependence was associated with an independent measurement of the fibre–matrix interfacial shear strength and was related to the degree of fibre–matrix reaction taking place during composite fabrication.

1. Introduction

The carbon fibre reinforced glass matrix composite system has potential industrial importance because it combines many of the attributes of polymer–matrix composites with the improved environmental stability and high-temperature resistance provided by glass matrices. The purpose of this investigation was to examine composite mechanical properties in the light of fibre, matrix and fibre–matrix interface characteristics. A recent companion study [1] has examined tensile performance as a function of orientation for uni- and bi-axially reinforced specimens.

Previous research on this system has demonstrated that high-strength composites can be fabricated using both continuous [2–11] and discontinuous carbon fibre reinforcements [12, 13]. In addition, composite dimensional stability [14, 15] and tribological characteristics [16, 17] appear to offer uniquely desirable characteristics. The range of applications seems to be limited most significantly by the progressive oxidation of the carbon fibres at elevated temperatures [18].

2. Experimental procedures

2.1. Composite fabrication

All composites were fabricated utilizing the tape-winding and hot-pressing procedure described previously [19]. The matrices were all obtained as −325 mesh size glass powders which were combined with water to produce slurries through which the carbon fibre tows could be pulled. The infiltrated carbon fibre tows were then wound on to a mandrel, dried and the final composite densified under pressures of 6.89 MPa at temperatures in excess of 1200° C.

The carbon fibre used in this investigation was the HMU type (Hercules Co.) having an elastic modulus of 380 GPa and a tensile strength of 2700 MPa. It was used in both 1000 and 3000 filaments per tow sizes. The principal glass used was a commercial borosilicate glass (Corning type 7740). Other borosilicate glasses used were custom-melted to provide desired fibre matrix reactions.

2.2. Mechanical testing

Mechanical test procedures included both three-point flexural testing and tensile testing. The flexural tests were performed only on unidirectionally reinforced composites. Flexural specimen geometry was varied to permit the ratio of maximum flexural stress to shear stress to be altered.

Tensile tests were performed using both parallel-sided specimens and reduced-section machined gauge-length specimens. The former were used for room-temperature testing of both uniaxially and multiaxially reinforced specimens, while the machined specimens were used for the high-temperature tensile testing of 0/90 reinforced samples. In both cases the gauge length was 2.5 cm and the loads were applied at a strain rate of 0.05 min^{-1}. At room temperature, strain measurements were made using glued-on strain gauges while at elevated temperature clip-on extensometry was used.

3. Results and discussion

3.1. Carbon fibre reinforced borosilicate mechanical properties

Uniaxial and 0/90 cross-ply composites of carbon fibre reinforced borosilicate 7740 glass were fabricated for testing in tension and flexure to determine composite overall stress–strain behaviour and failure modes.

3.1.1. Uniaxially reinforced composites

Typical single-cycle and double-cycle tensile stress–strain curves for a uniaxially reinforced HMU fibre-reinforced 7740 glass composite are shown in Fig. 1. The single-cycle curve was linear up to a strain of approximately 0.13% and a stress of 200 MPa. This point of deviation is referred to as the "proportional

0022–2461/88 $03.00 + .12

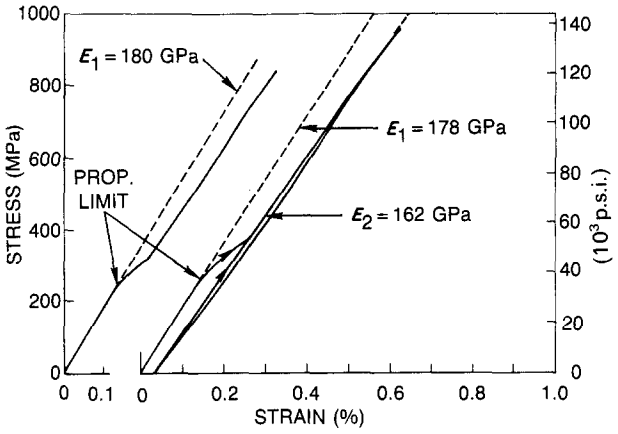

Figure 1 Single-cycle and double-cycle tension stress–strain curves for uniaxial 50% HMU fibre-reinforced 7740 glass.

limit" and marks the point at which matrix cracking and/or fibre–matrix debonding becomes prominent. Similar behaviour has been well documented in the Nicalon SiC fibre-reinforced LAS glass–ceramic composite system [20–22]. The fracture path for specimens of this type exhibited substantial shear along planes parallel to the fibres due to the very low off-axis strength of the composites. Higher-magnification views of the fracture surfaces also revaled a predominantly fibre pull-out mode of failure. The fibres are pulled free of the matrix due to the low interfacial strength, with the length of pull-out being in the range of approximately 3 to 10 times the fibre diameter.

By loading a specimen to 800 MPa, then unloading and then finally reloading to failure (Fig. 1), it was possible to reveal a permanent decrease in elastic modulus (from 178 to 162 GPa) which occurred due to matrix cracking. Also of note for these specimens is a comparison in flexural and tensile behaviour (Fig. 2). The flexural strength is significantly greater and the flexure specimen fracture surface exhibits significantly longer fibres pulled free of the matrix. The dramatic difference in fracture behaviour is due to the presence of both interlaminar shear (which frees fibres from the matrix) and tensile stresses in the flexure test. In addition a very large deflection was necessary to fracture the flexure specimen after test so that the fracture surface could be examined.

Flexural testing was performed over a range of span (L) to depth (h) ratios for a second set of specimens containing a lower fibre content. Specimens of two orientations were tested (Fig. 3). The difference between these specimens has to do with the orientation of the original tape plys relative to the direction of applied load. The applied load–mid-span deflection trace shown in Fig. 4 is typical of those obtained. Again, a linear region occurred initially, followed by a very jagged curve. The test was generally discontinued after it was clear that the maximum load-carrying capability of the specimen has been passed. At this point, however, specimen failure had not occurred and the inherent crack growth resistance of this composite prevented ultimate fracture. Using the proportional limit and maximum load points shown on this curve and from curves of other specimen tests, it has been possible to plot the maximum applied shear stress (stress at the midplane of the specimen) as a function of specimen span-to-depth ratio (Fig. 5). In all but the highest L/h cases the stresses associated with the proportional limit and the maximum load are plotted. In the highest L/h tests the load–deflection curves were not obtained and a proportional limit was thus not measured. The data are represented in terms of shear stress rather than flexural stress due to the fact that nearly all the specimens exhibited shear as their primary mode of failure. At the higher L/h ratios compression failure was also noted and only at the highest L/h ratio of 25 was there evidence of tensile failure.

In the case of the "interlaminar" orientation specimens, the data for the smallest span-to-depth ratio tests (L/h = 4) are associated with specimens whose cut ends clearly show the evidence of interlaminar shear cracks (Fig. 6). By looking at this specimen end at this magnification it is possible to see that the shear plane is primarily along the fibre–matrix interface, moving from fibre to fibre.

By testing flexural specimens in an "edge-on" orientation it was found that composite shear strength was markedly increased. The two different specimen orientations shown in Fig. 3 make evident the reason for the higher shear strength due to the loss of easy

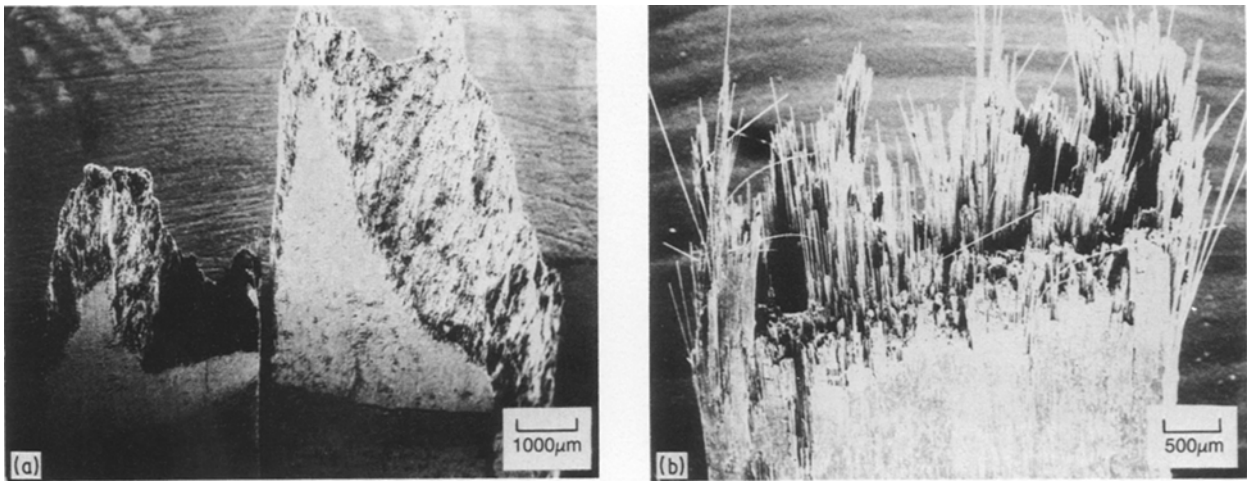

Figure 2 Comparison between tension and flexure behaviour for uniaxial HMU fibre-reinforced 7740 glass: (a) tensile, UTS = 839 MPa (122 ksi); (b) flexure, σ = 1150 MPa (166 ksi).

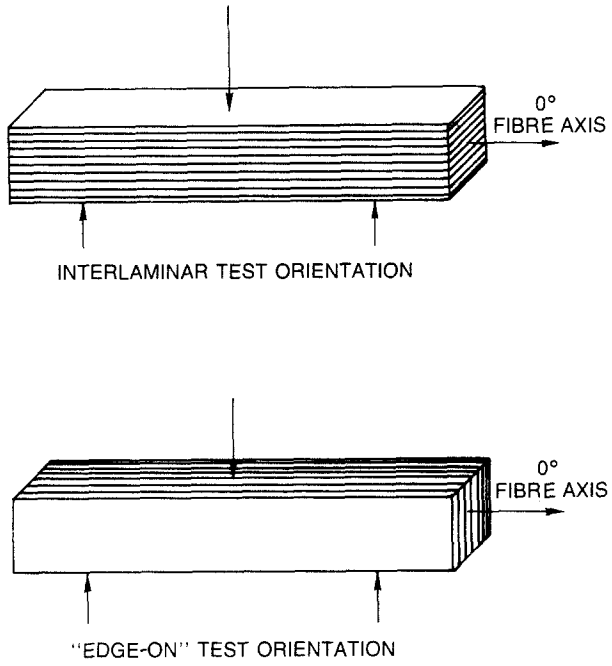

Figure 3 Three-point flexure specimen orientations tested. The lay-up of the plys is shown relative to the specimen three-point loading scheme.

interlaminar planes for shearing. Examination of the edge-on specimens after test was unable to reveal any interlaminar cracks such as those shown in Fig. 6. Thus the original plys have left clearly defined regions of weakness for shear failure in the interlaminar specimens.

Based primarily on the data taken from the shortest-span tests it was concluded that the interlaminar shear strength of these composites was approximately 22 MPa. The edge-on oriented specimens failed at the significantly higher maximum shear stress of 33 MPa. It is interesting to note that this value of 33 MPa is in good agreement with the value of shear strength used to accurately predict the off-axis tensile strength of similar composites using the Tsai–Hill failure criteria [1]. In this related case, a shear strength of 32 MPa was successfully used to predict the strength of both unidirectional and angle-ply composites.

3.1.2. Cross-ply reinforced composites

Cross-ply reinforced (0/90) tensile specimens were fabricated having nearly the same fibre content as the

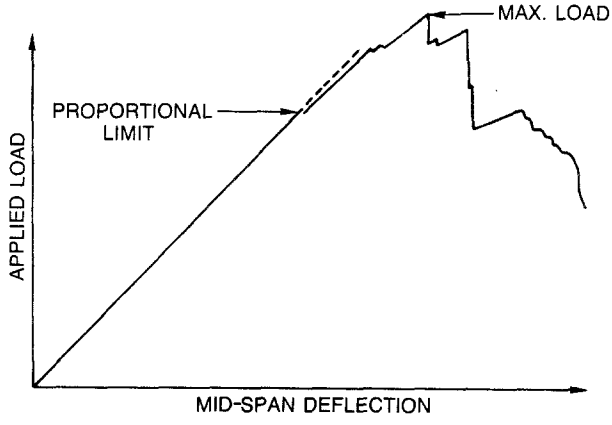

Figure 4 Typical applied load–mid-span deflection curve for uniaxial HMU-reinforced 7740 glass.

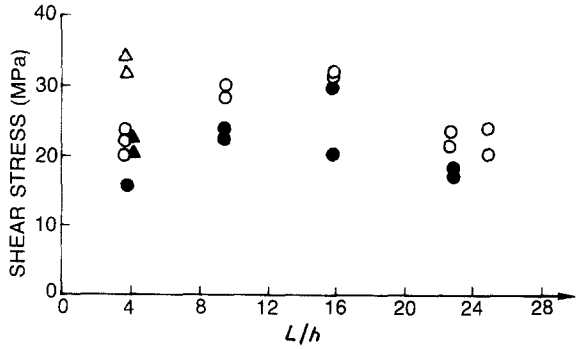

Figure 5 Calculated maximum mid-plane shear stress as a function of test span (L) to depth (h) ratio for uniaxial 38 vol % HMU fibre-reinforced 7740 glass. (○, △) Based on maximum load; (●, ▲) based on proportional limit. (○, ●) Interlaminar orientation; (△, ▲) edge-on orientation.

uniaxial specimens. The tensile stress–strain curve for a typical specimen is shown in Fig. 7. The summary of composite strength and elastic modulus for 0° and 0/90 specimens fabricated under identical conditions is presented in Table I. The 0/90 composite elastic modulus was measured to be half that of the uniaxial composites, indicating that the 90° plies contribute almost nothing in stiffness. In contrast, however, the 0/90 composites were less than half the strength of the uniaxial composites, indicating that the 0° plies are apparently weakened by the presence of the 90° plies when tested in this configuration.

The proportional limit stress for the 0/90 composites was found to be extremely low due to the fact that 90° ply cracking occurs at very low strain levels.

The fractured 0/90 tensile specimens exhibited more planar fracture on the macro-scale because the 90° plies prevented the large shear cracks parallel to the 0° direction from forming as noted in the unidirectionally reinforced specimens. On the other hand, high-magnification examination of the 0/90 composite fractures (Fig. 8) revealed more extensive pull-out than in the unidirectional case alone. This is probably due to the number of fibres at the 0/90 interply boundaries that are less well surrounded by glass, and also the probability of much greater matrix cracking in the 90° plies freeing up adjacent 0° fibres.

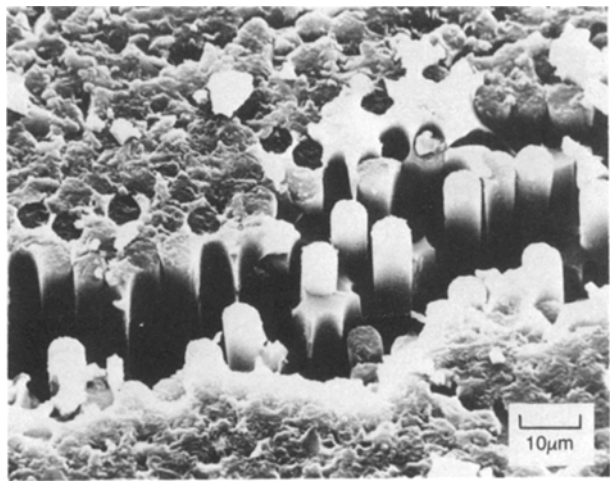

Figure 6 Cut flexural specimen edge after testing, revealing path of shear crack along fibre–matrix interface.

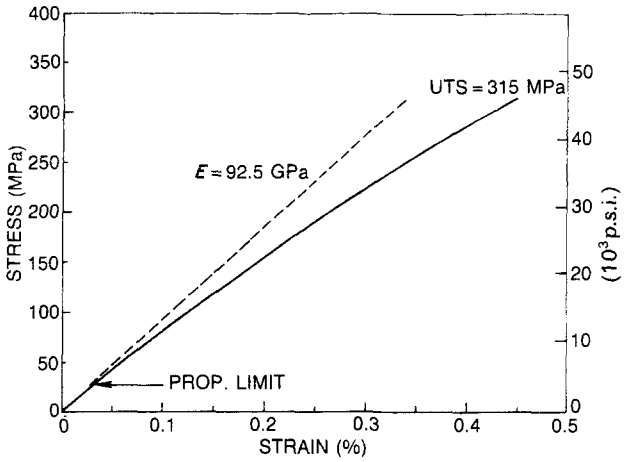

Figure 7 Tension stress–strain curve for 0/90 52 vol % HMU fibre-reinforced 7740 glass.

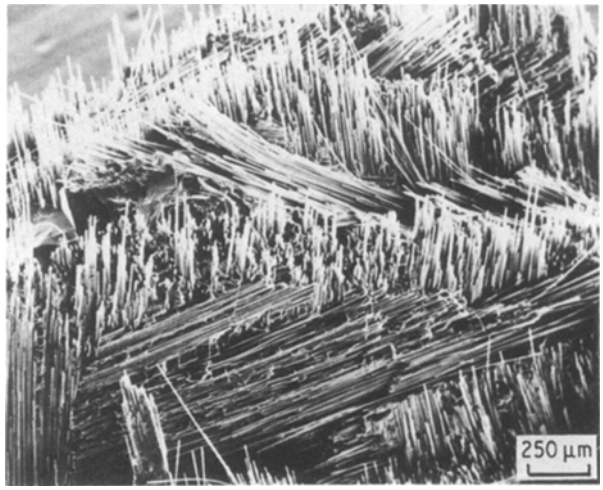

Figure 8 0/90 reinforced tensile specimen fracture surface.

3.1.3. Elevated-temperature tensile strength of cross-ply reinforced composites

A series of 0/90 reinforced HMU/7740 composites was fabricated to permit the determination of tensile strength as a function of test temperature. The 0/90 orientation was chosen so that tensile specimens with a reduced gauge section could be used for test without causing extensive shear parallel to the fibres. All tests were performed in air with a hold-time at temperature prior to test of less than 10 min to minimize the deleterious effects of oxidation.

The resultant properties are listed in Table II. While elastic modulus is relatively independent of temperature, composite tensile strength decreased significantly above 540° C, which is close to the borosilicate glass matrix annealing point (Fig. 9). Due to the short time of exposure to temperature it was not anticipated that a significant reduction in strength would have occurred due to oxidation of the carbon fibres at even 600° C. The decrease in composite proportional limit at above 540° C also points to an important contribution of matrix to the failure mechanism. It is also of interest that, while composite strength decreased substantially at 625° C, the composite ultimate failure strain was much less temperature-dependent. The fact that these composites exhibited significantly higher proportional limit stresses than that presented in Table I may be due to the use of a less sensitive extensometry system for these samples. The extensometer was necessary to permit strain measurement at elevated temperature.

TABLE I Tensile performance comparison for HMU fibre-reinforced 7740 composites (both hot-pressed under identical conditions)

Orientation	Fibre content (vol %)	UTS (MPa)	Proportional limit (MPa)	E (GPa)	ε_f (%)
0°	50	839	180	180	0.54
		953	200	178	0.63
0/90	52	289	14.6	90.7	0.44
		308	18.1	87.1	0.50
		315	15.8	92.5	0.45

3.1.4. Effect of fibre content on uniaxially reinforced composites

A series of uniaxially reinforced composites was fabricated to evaluate the effect of fibre content on composite stress–strain behaviour and shear properties. Two different fibre tow sizes were used in composite fabrication to examine their effects on performance.

The tensile stress–strain curves for three of the specimens fabricated with 1000-filament tows are shown in Fig. 10. As can be seen from the curves, there has been a significant change in stress–strain behaviour with change in fibre content. The composite elastic modulus E_c obtained from the initial linear portions of the curves increased with increasing fibre content V_f. The data, taken from Fig. 10 and also Table III, are all plotted in Fig. 11. The best-fit straight line corresponds to a rule of mixtures projection (Equation 1 below) that extrapolates to an effective fibre elastic modulus E_f of 310 MPa, which is significantly less than the value of 380 MPa associated with the fibre by the manufacturer. The projected matrix modulus E_m of 55 MPa is in fair agreement with the 63 MPa associated with the unreinforced

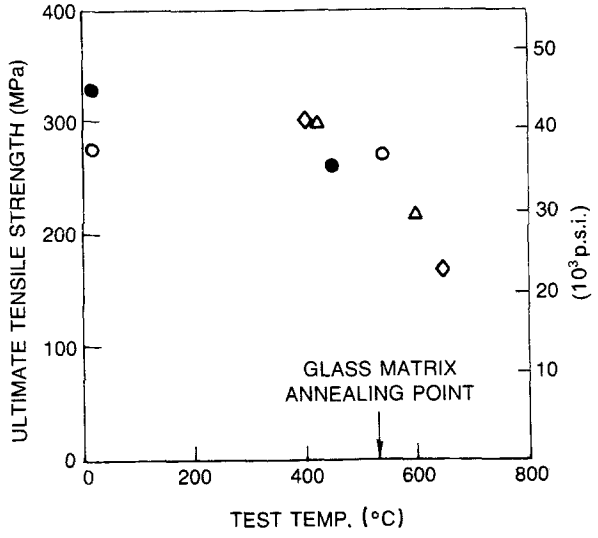

Figure 9 Ultimate tensile strength of 0/90 HMU fibre-reinforced 7740 glass at temperature in air. Similar symbols designate samples taken from a single composite plate.

TABLE II 0/90 HMU/7740 composite tensile properties measured at temperature in air

Fibre content (vol %)	Test temperature (%)	UTS (MPa)	Proportional limit (MPa)	E (GPa)	ε_f (%)
42	25	328	52	–	0.47
42	450	259	49	72	0.44
47	25	276	85	83	0.42
47	540	269	38	91	0.47
38	403	303	75	75	0.48
38	625	168	30	66	0.40
39	425	301	62	82	0.46
39	600	222	27	70	0.44

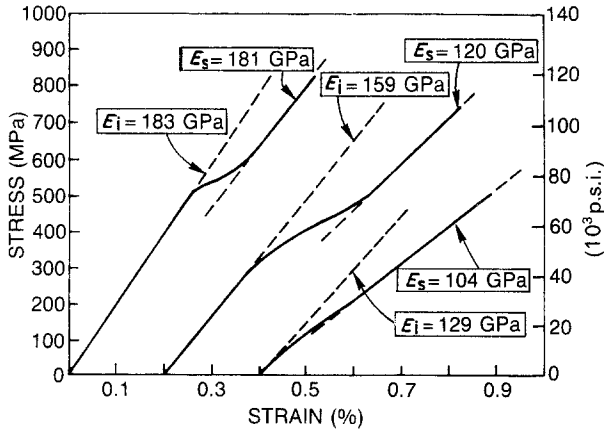

Figure 10 Effect of fibre content on the tensile stress–strain behaviour for uniaxial HMU fibre-reinforced 7740 glass. Fibre contents are from left to right 55, 40 and 29 vol %.

matrix. Microcracks present in the matrix after fabrication would tend to reduce the value somewhat.

$$E_c = E_f V_f + E_m V_m \quad (1)$$

As would be expected, composite tensile strength increased significantly with fibre content, and the stress associated with the composite proportional limit increased even more rapidly (Fig. 12). Another way of examining these data is to look at the composite strain levels associated with these stresses (Fig. 13). The failure strain of the composite is nearly constant at 0.5% and independent of fibre content, indicating that the strength increases observed were primarily due to increases in fibre content. In contrast, the strain levels associated with the proportional limit increased significantly, most probably due to a refinement of the structure and mechanisms relatable to the Aveston–Cooper–Kelly (ACK) model [23–25]. The ACK model predicts that the matrix cracking strain increases with fibre content according to the relationship

$$\varepsilon_m = \left(\frac{12\tau\gamma_m E_f V_f^2}{E_c E_m^2 r V_m} \right)^{1/3} \quad (2)$$

where ε_m = matrix failure strain in the composite at proportional limit, E = elastic moduli of composite, matrix or fibre, τ = interfacial shear strength, V = volume fractions, r = fibre radius and γ_m = matrix surface fracture energy.

Because the elastic modulus of the composite, E_c, is dominated by the term $E_f V_f$ in Equation 1, it is expected that the dependence of ε_m or V_f can generally be approximated by a $V_f^{1/3}$ term. Also of note is the fact that the 1000 filament per tow fibre-reinforced composites exhibited significantly higher proportional limit stresses and strains, probably because of a more uniform fibre distribution as compared to the much larger 3000-fibre tow reinforced samples. The tow size had much less of an effect on ultimate strength, reflecting a lesser dependence on microstructural distribution for this property.

Comparison of macroscopic fracture modes for the 1000-filament reinforced composites (Fig. 14) demonstrates a significant change in failure mode with fibre content. As fibre content increased, the composite failure mode became more and more irregular. Closer examination of the specimen fracture surfaces revealed a wide range of fracture characteristics. In one region (Fig. 15) very long fibre pull-out was observed and

TABLE III Effect of fibre content on 0° HMU/7740 composite properties

Fibre tow size*	Fibre content (vol %)	Tensile test					Short-beam shear strength (MPa)	
		UTS (MPa)	ε_f (%)	E (GPa)	Proportional limit (MPa)	Proportional limit strain (%)	Interlaminar	Edge-on
1K	29	507	0.49	129	53.0	0.04	39.6	51.1
		466	0.48	127	46.8	0.04	40.3	52.1
1K	35	436	0.40	156	192	0.12	–	–
		540	0.52	156	173	0.11	–	–
1K	40	734	0.57	158	283	0.18	40.9	44.6
		724	0.62	159	304	0.19	42.3	–
1K	55	826	0.52	193	499	0.26	–	–
		837	0.51	198	453	0.23	–	–
3K	38	592	0.50	144	72	0.05	22.2	33.0
		555	0.44	145	70	0.05	–	–
3K	54	–	–	–	–		32.9	44.4
		–	–	–	–		29.9	–
3K	50	839	0.54	180	180	0.10	–	–
		953	0.63	178	200	0.11	–	–

*Number of filaments per two 1K = 1000, 3K = 3000.

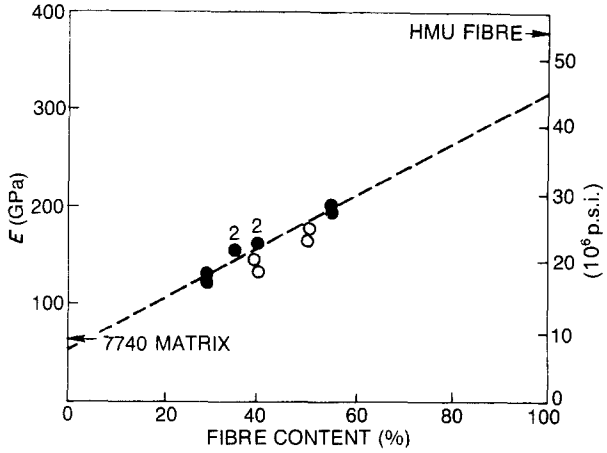

Figure 11 Elastic modulus of uniaxial HMU fibre-reinforced 7740 glass: (●) 1000-filament tows, (○) 3000-filament tows.

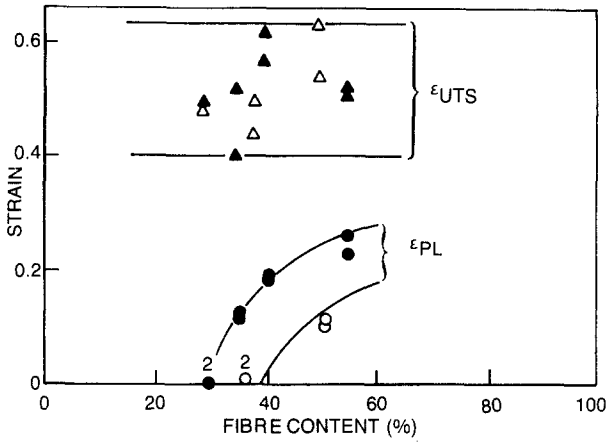

Figure 13 Tensile failure strain and proportional limit strain for the same composites as in Fig. 12.

seems to be associated with a relatively high fibre content. In another region, both fibre content and the degree of fibre pull-out were significantly lower. The lesser degree of pull-out appears associable with a lower fibre content.

3.1.5. Effects of matrix composition

The borosilicate glass matrix used in the previously described portions of this report consisted of a standard composition of the Corning Glass Works designated 7740. It was the purpose of this portion of the investigation to fabricate composites with other controlled compositions of glass to determine the effects of chemistry and fibre–glass reactions on composite properties. In particular, it was planned that controlled fibre–matrix reactions would take place during composite fabrication to alter the composition and properties of the fibre–matrix interface and to determine the effects of these changes on composite mechanical properties. The analysis of potential fibre–matrix reactions is described in detail elsewhere [26], while the matrix compositions selected for composite fabrication, as well as the standard 7740 glass, are listed in Table IV. It should be noted that the changes in matrix chemistry were made in such a way as to minimize changes in matrix physical properties such as thermal expansion and stiffness.

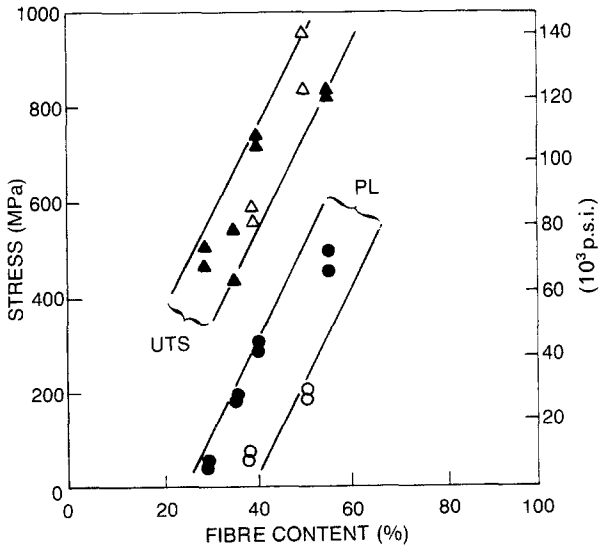

Figure 12 Tensile strength (UTS) and proportional limit stress (PL) for uniaxial HMU fibre-reinforced 7740 glass: (●, ▲) 1000-filament tows, (○, △) 3000-filament tows.

As a starting point, the surface chemistry of the as-received HMU fibre was compared with that of fibres in a 7740 glass matrix composite. The as-received fibre surface was very smooth and scanning Auger microscopic (SAM) analysis revealed the fibre chemistry to be 100% carbon down to 100 nm into the fibre surface. In contrast the chemistry of the fibres located on the fracture surface of a 7740 matrix composite contained evidence of both silicon and oxygen diffusion into the fibre. Analysis of the matrix surface out of which a neighbouring fibre had been pulled during composite fracture also revealed extensive diffusion of carbon into the glass matrix.

The series of uniaxially reinforced composites fabricated out of the trial matrices is listed in Table IV. Each of these compositions was used to make thin samples for tensile testing and thicker ones for short-beam shear testing. Composite tensile strength was affected significantly by matrix composition with the molybdenum-containing glass exhibiting a significant strength reduction. This was also associated with a definite decrease in fibre pull-out length. Close examination of the surfaces of fibres on the fracture surface of this molybdenum-containing composite also revealed evidence of fibre–matrix reaction. An independent measure of the presence of this reaction and its affect on the fibre–matrix interface was obtained by applying a load to individual fibre ends and measuring the stress necessary to initiate debonding of the fibre from the matrix [27]. The resultant fibre–matrix interfacial shear stress was obtained using the applied load necessary to cause the observed initial debond in a finite-element stress analysis. The obtained interfacial strength data were associated with the interlaminar short-beam shear strength (SBSS) measured on specimens from the same composite samples. These data (Fig. 16) indicate that an interfacial bond strength increase can be associated with an increase in short-beam shear strength. This is in agreement with the model proposed by Phillips [5] and the observed fracture mode for short beam shear (Fig. 6) which showed shear cracks following the fibre–matrix interfacial regions.

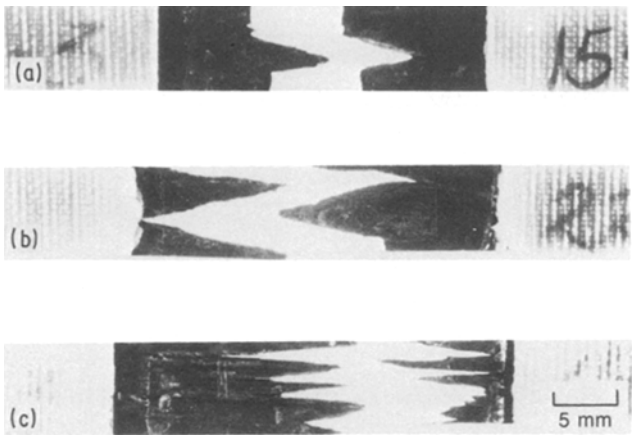

Figure 14 Fractured tensile specimens of uniaxial HMU fibre-reinforced 7740 glass with (a) 29, (b) 40 and (c) 55 vol % fibre reinforcement.

4. Summary

Carbon fibre reinforced glass matrix composites have been shown to be high-strength, high-stiffness materials whose performance can be related to their constituent properties and the role of the fibre–matrix interface. Composite tensile strengths of nearly 1000 MPa, combined with an axial elastic modulus of 180 GPa and an overall composite density of 2 g cm^{-3}, make these composites important candidates for structural applications. The shape of the composite tensile stress–strain curves is strongly dependent on the level of proportional limit stress. After this stress has been exceeded the composite stiffness is reduced significantly, most probably by the occurrence of matrix cracking and also the debonding of the fibre surface from the matrix. Both of these occurrences will cause an irreversible reduction in composite axial elastic modulus.

The retention of composite tensile strength to 540° C is also notable in that, while limited by carbon fibre oxidation, it provides significant potential advantage over traditional polymer and aluminium matrix composites.

Comparison with polymer matrix composites is also relevant in that it points to a potential degradation of fibre properties during the glass matrix composite fabrication process. An epoxy matrix composite made as part of this investigation using approximately 50% by volume of the same HMU type fibres exhibited a tensile strength of 1500 MPa. This is 50% greater than the herein reported glass matrix composite tensile strengths, and points to a significant loss of fibre performance. As reported in this paper, the effective fibre elastic modulus obtained for these composites (Fig. 11), is also reduced significantly below that reported by the fibre producer and again points to fibre degradation.

The role of fibre–matrix reaction was investigated somewhat further and shown to be significantly altered through the use of matrices containing reactive elements. Enhanced reaction reduced the effective fibre strength even further, but at the same time increased the composite shear strength. This points to the dilemma facing those wishing to develop optimized fibre-reinforced ceramic matrix composites. To

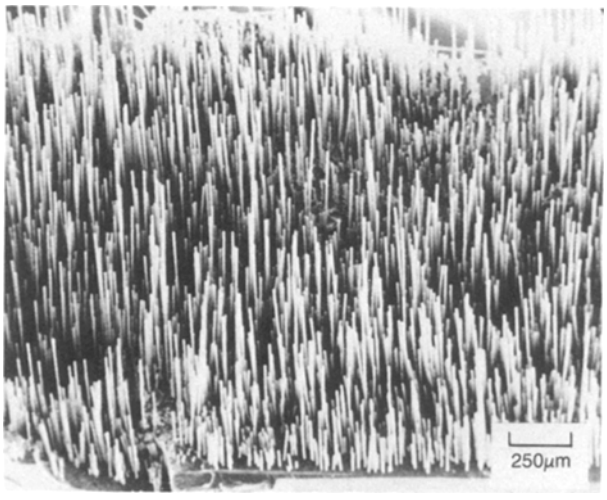

Figure 15 High fibre pull-out region of a uniaxial HMU fibre-reinforced 7740 glass composite containing 29 vol % fibre.

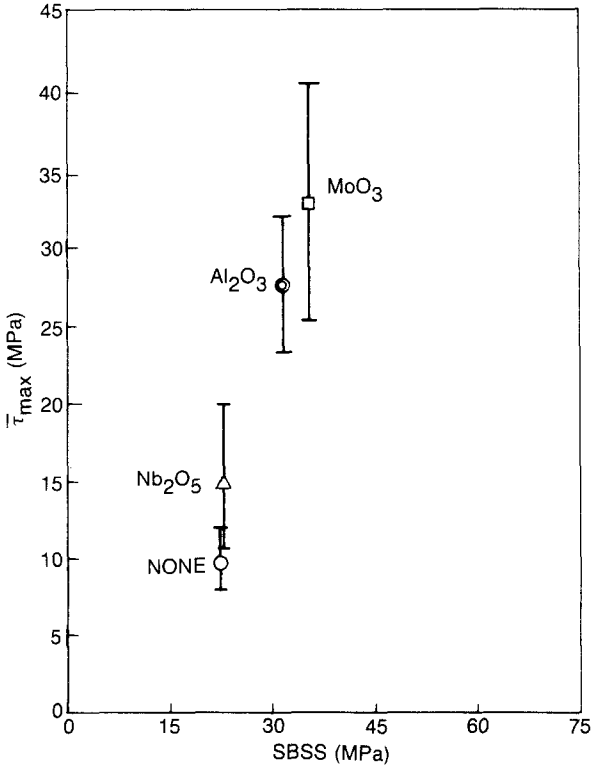

Figure 16 Fibre–matrix interfacial debond shear strength (τ_{max}) against composite short-beam shear strength (SBSS) for uniaxial HMU fibre-reinforced borosilicate glasses containing the additions indicated.

TABLE IV Effect of matrix composition on composite tensile properties

Matrix Composition (wt %)*	Fibre content (vol %)†	UTS (MPa)	ε_f (%)	E (GPa)	Proportional limit (MPa)
82% SiO_2, 14% B_2O_3, 4% Na_2O	51	859	0.56	188	474
		814	0.52	193	445
81% SiO_2, 14% B_2O_3, 4% Na_2O, 1% Nb_2O_5	42	971	0.67	173	352
		904	0.64	179	271
81% SiO_2, 14% B_2O_3, 4% Na_2O, 1% MoO_3	44	569	0.33	175	490
		557	0.34	179	330

*7740 Composition is 81% SiO_2, 13% B_2O_3, 4% Na_2O, 2% Al_2O_3.
†3000-filament tows used.

preserve fibre strength and achieve a high degree of fracture toughness it is necessary to have a low fibre–matrix interfacial strength. This, however, results in low composite shear strength and also off-axis tensile strength. By increasing the fibre–matrix bond we increased shear strength but severely reduced tensile strength and toughness. In the future it will be necessary to achieve compromises between these two extremes based on the requirements of particular applications.

Acknowledgements

The author wishes to thank Professor Carlo Pantano of Pennsylvania State University for his assistance in the selection of the experimental glass compositions, Dr John Mandell of the Massachusetts Institute of Technology for the measurements of fibre–matrix interfacial shear strength, and Dr John Brennan of UTRC for the SAM analysis of fibre–matrix interface chemistry. The support of this investigation under the auspices of Dr S. Fishman, Office of Naval Research, is appreciated.

References

1. V. NARDONE and K. M. PREWO, *J. Mater. Sci.* **23** (1988) 168.
2. R. A. SAMBELL, A. BRIGGS, D. C. PHILLIPS and D. H. BOWEN, *ibid.* **7** (1972) 676.
3. D. C. PHILLIPS, R. A. SAMBELL and D. H. BOWEN, *ibid.* **7** (1972) 1454.
4. S. R. LEVITT, *ibid.* **8** (1973) 793.
5. D. C. PHILLIPS, *ibid.* **9** (1974) 1847.
6. K. M. PREWO and J. F. BACON, in Proceedings of 2nd International Conference on Composites, edited by B. Noton (AIME, New York, 1978).
7. K. M. PREWO, J. F. BACON and E. R. THOMPSON, in Proceedings of AIME Conferences on Advanced Fibres and Composites for Elevated Temperatures, edited by I. Ahmad and B. Noton (1979).
8. K. M. PREWO and E. R. THOMPSON, "Research on Graphite Reinforced Glass Matrix Composites", NASA Contract Report 165711 (Hartford, Connecticut, 1981).
9. K. M. PREWO, J. F. BACON and D. L. DICUS, *SAMPE Q.* **10** (4) (1979) 42.
10. K. M. PREWO and E. J. MINFORD, *SAMPE J.* **21–22** (1985).
11. M. SAHEBKAR, J. SCHLICHTING and P. SCHUBERT, *Ber. Deutsch. Keram. Gasell.* **55** (1978) (5) 265.
12. R. A. SAMBELL, D. BOWEN and D. C. PHILLIPS, *J. Mater. Sci.* **7** (1972) 663.
13. K. M. PREWO, *ibid.* **17** (1982) 3549.
14. *Idem,* in Proceedings of Special Topics in Advanced Composites Meeting, El Segundo (1979) p. 1–30.
15. K. M. PREWO and E. J. MINFORD, *Proc. SPIE – Int. Soc. for Opt. Engnrs* **505** (Aug. 1984) p. 188–91.
16. V. D. KHANNA and Z. ELIEZER, in Proceedings of Conference on the Mechanical Behaviour of Metal Matrix Composites, edited by J. Hack (AIME, Dallas, Texas, 1983) p. 227–34.
17. E. MINFORD and K. PREWO, *Wear* **102** (1985) 253.
18. K. M. PREWO and J. A. BATT, *J. Mater. Sci.* in press.
19. K. M. PREWO, J. J. BRENNAN, G. K. LAYDEN, *Ceram. Bull.* **65** (2) (1986) 305.
20. K. M. PREWO, "Advanced Characterization of SiC Fibre Reinforced Glass–Ceramic Matrix Composites", Office of Naval Research Contract N00014-81-C-0571 Report 83-915939 (Hartford, Connecticut, 1983).
21. D. M. MARSHALL and A. G. EVANS, *J. Amer. Ceram. Soc.* **68** (5) (1985) 225.
22. K. M. PREWO, *J. Mater. Sci.* **21** (1986) 3590.
23. J. AVESTON, G. A. COOPER and A. KELLY, in Proceedings of Conference on the National Physical Laboratory, UK (IPC, England, 1971).
24. J. AVESTON and A. KELLY, *J. Mater. Sci.* **8** (1973) 352.
25. D. B. MARSHALL, B. N. COX and A. G. EVANS, *Acta Metall.* **33** (1985) 2013.
26. P. M. BENSON, K. E. SPEAR and C. C. PANTANO, in Proceedings of Ceramic Microstructures '86 Conference, edited by J. Pask (Plenum, 1988).
27. J. F. MANDELL, private communication (1987).

Received 4 August
and accepted 22 October 1987